

MICROSTRUCTURE OF SWIFT HEAVY ION IRRADIATED MgAl_2O_4 SPINEL

S.J. ZINKLE*, H.J. MATZKE** AND V.A. SKURATOV***

*Oak Ridge National Laboratory, P.O. Box 2008, Oak Ridge, TN 37831-6376 USA, zinklesj@ornl.gov

**EC, JRC, Institute for Transuranium Elements, P.O. Box 2340, D-76125 Karlsruhe, Germany

***Joint Institute for Nuclear Research, Flerov Lab, 141980 Dubna, Russia

ABSTRACT

Plan view and cross-section transmission electron microscopy was used to investigate the microstructure of magnesium aluminate spinel (MgAl_2O_4) following room temperature irradiation with either 430 MeV Kr, 614 MeV Xe, or 72 MeV I ions. The fluences ranged from $1 \times 10^{16}/\text{m}^2$ (single track regime) to $1 \times 10^{20}/\text{m}^2$. Destruction of the ordered spinel crystal structure on both the anion and cation sublattices was observed in the ion tracks at low fluences. At intermediate fluences, the overlapping ion tracks induced the formation of a new metastable crystalline phase. Amorphization with a volumetric expansion of ~35% was observed in spinel irradiated with swift heavy ions (electronic stopping powers >7 keV/nm) at fluences above $1 \times 10^{19}/\text{m}^2$. These results demonstrate that swift heavy ion radiation can induce microstructural changes not achievable with conventional elastic collision irradiation at comparable temperatures.

INTRODUCTION

MgAl_2O_4 is under consideration for insulator applications in proposed fusion reactors [1,3] and as an inert matrix host for fission reactor fuels [4]. Numerous neutron [1,3,5] and electron [6,7] irradiation studies have concluded that spinel has very good resistance to radiation damage. The radiation resistance of MgAl_2O_4 has been attributed to several factors, including crystal structure, efficient point defect recombination, relatively large size of the smallest stoichiometric defect cluster, high stability of faulted loops (which impedes loop unfauling and evolution to a network dislocation structure), efficient site exchange of different cations, and low interstitial migration energies [1,3,5,8].

Variable behavior has been reported for ion irradiated MgAl_2O_4 [8-13]. At temperatures ≥ 300 K, defect accumulation in spinel is dependent on the irradiation spectrum, with very limited defect cluster formation observed for light ion irradiations and pronounced cluster formation observed for heavy ion irradiations [8-10]. This has been interpreted as evidence for ionization- or subthreshold-displacement-induced diffusion, which would promote point defect recombination for low energy primary knock atoms. Formation of a disordered crystalline phase [12,14] and amorphization at higher doses [12] has been reported in some MgAl_2O_4 cryogenic ion irradiation studies. Amorphization has not been observed in MgAl_2O_4 irradiated at room temperature for doses up to ~100 displacements per atom (dpa) [11,15]. Amorphization of spinel at cryogenic temperatures (in the absence of implanted ion effects) requires temperatures below ~100 K and damage levels in excess of ~20 dpa for medium-energy (<12 MeV) ions [12,13,16,17].

Numerous studies have shown that discontinuous track formation in ceramic insulators can be produced by swift heavy ions with electronic stopping powers (dE/dx) above ~5 to 8 keV/nm, and continuous cylindrical tracks are typically observed for (dE/dx) ≥ 15 to 20 keV/nm [18]. The physical mechanism(s) responsible for track formation in radiolysis-resistant solids are still under debate (e.g., thermal spike vs. Coulomb explosion models). Therefore, additional data on a wide range of materials are needed to investigate material parameters such as the effect of band gap energy and thermal conductivity on track radius, etc. Of particular significance for the present study is the possibility that densely ionizing fission tracks (e.g. ~70 MeV I, Xe or Cs) can create irradiated microstructures that are not achievable with conventional (elastic collision) irradiations. If this is correct, then materials which exhibit good radiation resistance under elastic collision damage conditions (e.g., MgAl_2O_4) may not necessarily exhibit similar radiation damage resistance under fission track recoil conditions. This would be of importance for selection of candidate inert matrix fuel hosts for fission reactors, due to the large number of fission track recoils in reactor fuels.

DISCLAIMER

This report was prepared as an account of work sponsored by an agency of the United States Government. Neither the United States Government nor any agency thereof, nor any of their employees, make any warranty, express or implied, or assumes any legal liability or responsibility for the accuracy, completeness, or usefulness of any information, apparatus, product, or process disclosed, or represents that its use would not infringe privately owned rights. Reference herein to any specific commercial product, process, or service by trade name, trademark, manufacturer, or otherwise does not necessarily constitute or imply its endorsement, recommendation, or favoring by the United States Government or any agency thereof. The views and opinions of authors expressed herein do not necessarily state or reflect those of the United States Government or any agency thereof.

DISCLAIMER

Portions of this document may be illegible in electronic image products. Images are produced from the best available original document.

Although there have been several irradiation studies on the microstructure of magnetic insulators with the spinel crystal structure, there is only limited microstructural information on swift heavy ion irradiated MgAl_2O_4 [19,20]. Track formation (2.0-2.6 nm diameter) and octahedral cation disordering was observed in MgAl_2O_4 for $(dE/dx)_e \sim 20$ keV/nm, and the track diameter increased at higher $(dE/dx)_e$. Results obtained from further examination of the specimens from ref. [19] are described in the following sections, along with data from specimens [20] irradiated to significantly higher fluences.

EXPERIMENTAL PROCEDURE

Polycrystal and single crystal MgAl_2O_4 specimens were irradiated at room temperature with several different types of swift heavy ions. In one set of experiments, MgAl_2O_4 specimens were irradiated at the Dubna U-400 cyclotron facility with 430 MeV Kr or 614 MeV Xe ions to fluences of $\sim 1 \times 10^{16}$ ions/m² (isolated track regime). In a second set of experiments, MgAl_2O_4 specimens were irradiated at the Chalk River TASC irradiation facility (Atomic Energy of Canada Ltd.) with 72 MeV I ions (typical fission recoil ions) to fluences of 10^{18} to 10^{20} ions/m² (overlapping track regime, equal to $\sim 10^{24}$ - 10^{26} fissions/m³). The electronic stopping power and displacement damage profiles were calculated using the TRIM96 program [21]. Figure 1 shows the calculated results for 72 MeV ion irradiation. Table 1 summarizes the irradiation conditions for the various ions.

Following irradiation, cross-section TEM specimens were prepared by gluing the irradiated disks to polished unirradiated disks, sectioning, grinding to 0.1 mm, dimpling to 20 μm , and then dual-gun ion beam thinning at ~ 80 K with 6 keV Ar ions until perforation occurred near the interface. One specimen was also prepared using conventional plan-view (backthinning) techniques. The specimen surfaces were cleaned using 3 keV Ar ions at an angle of 11° and then coated with a thin (~ 5 nm) layer of carbon prior to examination. The specimens were examined using conventional bright-field and dark-field imaging techniques in either a Philips CM-12 or CM-30 microscope operating at 120 and 300 kV, respectively.

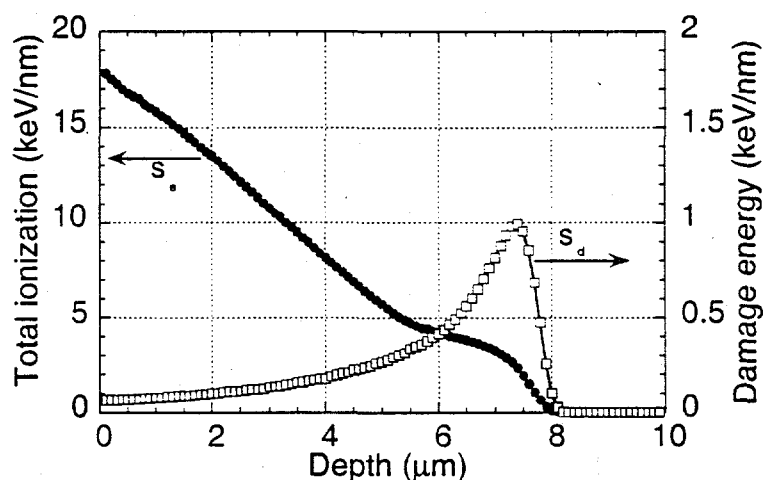


Fig. 1. Calculated damage energy (portion of nuclear stopping power that produces elastic collisions) and electronic stopping power for 72 MeV I ions in MgAl_2O_4 .

Table 1. Irradiation parameters for swift heavy ion irradiated MgAl_2O_4 .

Ion type	$(dE/dx)_e$ in investigated region	Damage Energy, S_d	Fluence (ions/m ²)	Displacements from elastic collisions (dpa)
430 MeV Kr	16 keV/nm	~ 0.01 keV/nm	$0.6-1.1 \times 10^{16}$	$\sim 1 \times 10^{-5}$
614 MeV Xe	26 keV/nm	~ 0.02 keV/nm	0.6×10^{16}	$\sim 2 \times 10^{-5}$
72 MeV I	< 18 keV/nm	0.1-1 keV/nm	$0.01-1 \times 10^{20}$	0.01-0.1 (low fluence) 1-10 (high fluence)

RESULTS

Figure 2 shows the plan view microstructure of MgAl_2O_4 irradiated with 430 MeV Kr ions to a low fluence, taken under weak dynamical ($s_g \sim 0.1 \text{ nm}^{-1}$) bright field imaging conditions. The white circular regions are due to strain contrast from individual ion tracks. The average diameter of the ion tracks taken under dynamical imaging conditions (3.0 nm) is slightly larger than the track diameter of $2.0 \pm 0.4 \text{ nm}$ based on octahedral cation disorder [19]. This suggests that the lattice strain may extend radially to distances that are greater than the disordered ion track core region. High-resolution lattice imaging of the plan view specimen did not reveal evidence for an amorphous core. As discussed elsewhere [19], a high density of small ($d \sim 3\text{-}5 \text{ nm}$) dislocation loops with $\{111\}$ habit planes were resolvable among the defect cluster debris at the periphery of individual ion tracks.

The possibility of disordering of the spinel structure within the ion tracks was investigated using centered dark field imaging. As shown in Fig. 3, dark ion tracks were visible in dark field images using diffraction vectors of $g = \langle 222 \rangle$ and $g = \langle 442 \rangle$. According to elastic scattering structure factor calculations, the intensity of the 222 diffraction spot in spinel is mainly determined by octahedral cations (tetrahedral cations do not contribute, and anions give a slight destructive contribution). Therefore, the dark ion track images in the top photo of Fig. 3 are evidence for disordering of the octahedral cations within the ion tracks (e.g., transfer to octahedral ions to tetrahedral sites). Since only oxygen ions contribute to the 442 electron structure factor of spinel, the dark ion track images in the bottom half of Fig. 3 imply that the anion spinel structure has been disrupted within the ion tracks. Additional analysis is needed to exclude the possibility that dynamical inelastic scattering may produce a contribution to the observed images.

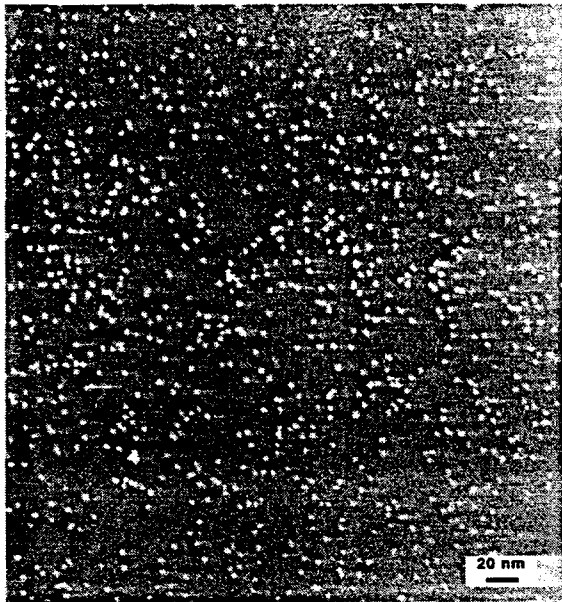


Fig. 2. Plan view of MgAl_2O_4 irradiated with 430 MeV Kr ions to a fluence of $6 \times 10^{15}/\text{m}^2$.

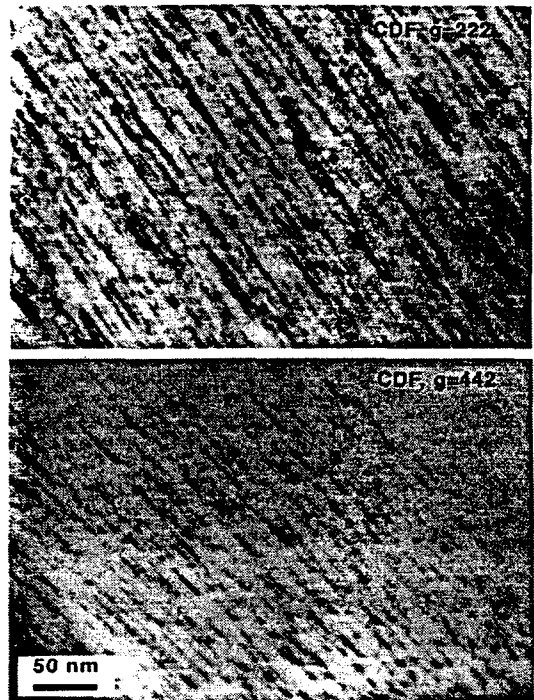


Fig. 3. Centered dark field images of MgAl_2O_4 irradiated with 430 MeV Kr ions to a fluence of $6 \times 10^{15}/\text{m}^2$. The specimen was tilted $\sim 10^\circ$ with respect to the electron beam direction (plan view specimen).

Swift heavy ion irradiation to higher fluences was performed using 72 MeV I ions (Table 1). After irradiation to a fluence of $1 \times 10^{18}/\text{m}^2$, partial transformation to a new crystal structure was evident in the irradiated regions extending up to a depth of $\sim 4.3 \mu\text{m}$. The new phase exhibited a pronounced weakening of the 111 and 220 diffraction spots. The irradiated microstructure at depths of $4.3\text{-}7.6 \mu\text{m}$ consisted of small defect clusters in a crystalline spinel lattice. From the TRIM calculations in Fig. 1, the transition from the metastable (radiation-induced) crystalline phase to the damaged spinel phase occurred for an electronic stopping power of $\sim 7.5 \text{ keV/nm}$. The new radiation-induced crystalline phase does not appear to be associated with conventional (elastic collision) displacement damage, since the new phase occurred at irradiated depths where the elastic collision damage was lowest ($< 0.025 \text{ dpa}$).

Irradiation of MgAl_2O_4 with 72 MeV I ions to a fluence of $1 \times 10^{20}/\text{m}^2$ produced an amorphous layer at depths up to $5.8 \mu\text{m}$, and a damaged crystalline spinel layer at depths of $5.8\text{-}9.1 \mu\text{m}$ (Fig. 4). According to Fig. 1, the calculated damage from elastic collisions in the amorphous region for this fluence was $< 3 \text{ dpa}$, whereas damage levels as high as 10 dpa existed in the crystalline damaged spinel region. Therefore, the amorphization appears to be associated with high electronic stopping power effects rather than elastic collision damage.

From a comparison of the depth-dependent microstructures of MgAl_2O_4 irradiated at different fluences, the swelling associated with the amorphization could be estimated. In particular, the subsurface damaged spinel band was $\sim 3.3 \mu\text{m}$ wide at both 1×10^{18} and $1 \times 10^{20}/\text{m}^2$, respectively. The near-surface metastable crystalline phase observed at $1 \times 10^{18}/\text{m}^2$ had a measured width of $4.3 \pm 0.1 \mu\text{m}$, and after a fluence of $1 \times 10^{20}/\text{m}^2$ this region transformed into an amorphous phase with a measured width of $5.8 \mu\text{m}$. Since the irradiated region is constrained in the lateral direction by the underlying unirradiated MgAl_2O_4 material, all of the volumetric swelling would occur in the direction normal to the surface. Therefore, the "step-height" linear swelling of $\Delta x/x = (5.8 - 4.3)/4.3$ corresponds to a volumetric swelling of $35 \pm 5\%$ for the crystalline to amorphous phase transformation in MgAl_2O_4 . This calculation assumes that the swelling associated with the transformation from the spinel structure to the metastable disordered crystalline phase is negligible.

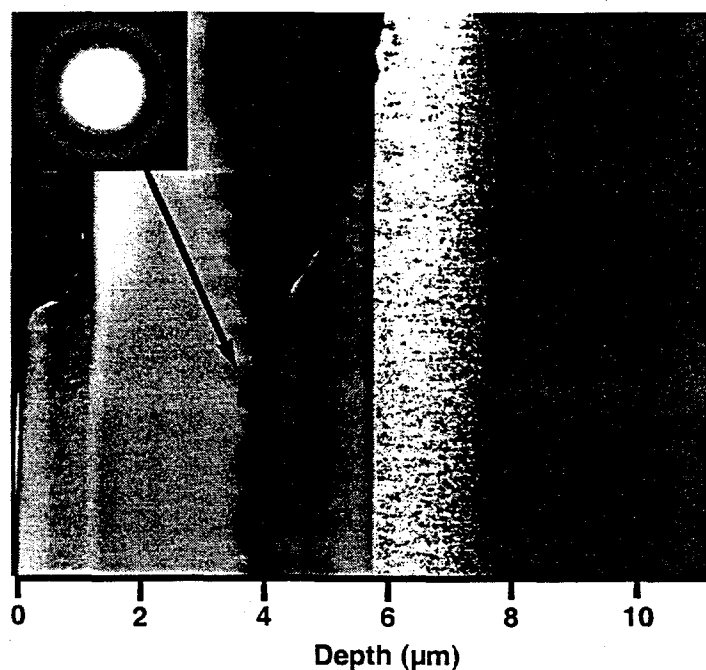


Fig. 4. Cross-section microstructure of MgAl_2O_4 irradiated to a fluence of 1×10^{20} ions/ m^2 .

DISCUSSION

The observed phase transformations in swift heavy ion irradiated MgAl_2O_4 appear to be due to high electronic stopping power effects rather than elastic collision processes. For example, the crystalline to amorphous transformation of MgAl_2O_4 irradiated with 72 MeV I ions to $1 \times 10^{20}/\text{m}^2$ (Fig. 4) occurred in the region with the lowest calculated displacement damage, <3 dpa. Previous room temperature ion irradiation studies using medium energy (<5 MeV) ions have not observed amorphization in MgAl_2O_4 for damage levels up to ~ 100 dpa [11,15]. The threshold level of electronic stopping power for inducing phase transformations in 72 MeV I ion irradiated MgAl_2O_4 at room temperature appears to be ~ 7.5 keV/nm. The sequence of phase transformations observed in the high electronic stopping power region of 72 MeV I ion irradiated MgAl_2O_4 (metastable crystalline phase formation, followed by amorphization) is similar to the behavior observed for MgAl_2O_4 irradiated at low temperature with medium energy ions [12,14]. A low-temperature ion irradiation study found that the elastic modulus of the metastable crystalline phase was $\sim 15\%$ higher than that of undamaged spinel, suggesting that some lattice strain was induced by the formation of the metastable phase [12].

A saturation swelling level of 22% was recently reported for 72 MeV I ion irradiated MgAl_2O_4 based on step-height measurements and assuming that the swelling occurred uniformly in the $8 \mu\text{m}$ irradiated region [20]. If these measurements are revised based on our observation that amorphization is induced only in the near-surface region ($x \leq 4.3 \mu\text{m}$), the estimated volume expansion due to amorphization of MgAl_2O_4 is $\sim 40\%$. A recent atomistic calculation [22] reported a swelling level of 31%. Both of these values agree with our TEM estimate, $\Delta V/V = 35 \pm 5\%$.

The microstructural observations from the present study indicate that amorphization of MgAl_2O_4 is not induced within the core of the swift heavy ion track for electronic stopping powers of 8-26 keV/nm. A similar lack of amorphization in the core of the swift heavy ion track has been reported for other radiolysis-resistant oxide ceramics such as MgO and Al_2O_3 for electronic stopping powers up to ~ 40 keV/nm [23-25]. Ion track amorphization has recently been reported for Al_2O_3 irradiated at $(dE/dx)_e = 62$ keV/nm [25]. Amorphization of MgAl_2O_4 at $(dE/dx)_e < 26$ keV/nm apparently requires an extended irradiation of the metastable phase; it would be interesting to investigate whether conventional ion irradiation of the metastable MgAl_2O_4 phase at room temperature would produce amorphization or conversion back to the spinel (Fd3m) phase. Work is in progress to identify the space group of the radiation-induced crystalline MgAl_2O_4 phase. Preliminary analysis of electron diffraction patterns (including whole-pattern convergent beam images) clearly indicates that the phase change is not simply a transformation from the cubic spinel structure (lattice parameter $a_0 = 0.808$ nm) to a cubic structure with a lattice parameter of $a_0 = 0.40$ nm, in contrast to previous suggestions [12,26].

For inert matrix fuel applications, it is important to investigate the temperature dependence of the swift heavy ion-induced phase transformations. The large volume change ($\sim 35\%$) associated with the crystalline to amorphous phase transition in MgAl_2O_4 may produce unacceptable stresses in fuel pin assemblies, depending on the detailed design. Recent work indicates that significant swelling occurs in MgAl_2O_4 during 72 MeV I ion irradiation at temperatures as high as 500°C , whereas swelling is not observed in specimens irradiated at $>900^\circ\text{C}$ [20]. The temperature range of interest for inert matrix fission reactor fuel applications is 400 - 1000°C . It is worth noting that a recent fission reactor irradiation of MgAl_2O_4 -matrix fuel containing 11 wt.% Am in finely dispersed microspheres produced a macroscopic swelling of 18% after fissioning $\sim 32\%$ of the Am at a calculated maximum temperature of $\sim 600^\circ\text{C}$ [27]. The measured swelling of 18% suggests that about half of the MgAl_2O_4 matrix may have become amorphous during the reactor irradiation, although swelling due to inert gas transmutation products may also be making a contribution.

CONCLUSIONS

Both the cation and anion sublattices of MgAl_2O_4 are disrupted by swift heavy ion tracks at room temperature for electronic stopping powers higher than a critical value of ~ 7.5 keV/nm. The disordered track diameter is ~ 2.5 nm for $(dE/dx)_e \sim 20$ keV/nm. There is no evidence for direct amorphization within the ion tracks for electronic stopping powers up to 26 keV/nm.

Swift heavy ion radiation can induce microstructural changes in MgAl_2O_4 not achievable with conventional elastic collision irradiation at comparable temperatures. Transformation to a

metastable crystal structure occurs at room temperature for moderate fluences of a representative fission fragment ion ($\sim 10^{19}/\text{m}^2$). Amorphization of the metastable crystal structure is induced at higher fluences ($\sim 10^{20}/\text{m}^2$). Further work is needed to investigate the temperature dependence of the swift heavy ion-induced phase transformations, particularly at elevated temperatures that are of interest for inert matrix fission reactor fuel applications.

Acknowledgements

The authors thank R.A. Verrall and P.G. Lucuta (TASCC accelerator facility, Chalk River, Canada) for arranging the 72 MeV I ion irradiations, and R.E. Stoller and I.M. Anderson for reviewing the draft manuscript. The TEM specimens were expertly prepared by J.W. Jones. This research was sponsored in part by the Office of Fusion Energy Sciences, U.S. Department of Energy under contract DE-AC05-96OR22464 with Lockheed Martin Energy Research Corp.

REFERENCES

1. F.W. Clinard, Jr., G.F. Hurley, and L.W. Hobbs, *J. Nucl. Mater.* **108&109**, 655 (1982).
2. G.P. Pells, *J. Nucl. Mater.* **155-157**, 67 (1988).
3. C. Kinoshita, K. Fukumoto, K. Fukuda, F.A. Garner, and G.W. Hollenberg, *J. Nucl. Mater.* **219**, 143 (1995).
4. Hj. Matzke, *Nucl. Instr. Meth. B* **116**, 121 (1996).
5. K.E. Sickafus, A.C. Larson, N. Yu et al., *J. Nucl. Mater.* **219**, 128 (1995).
6. S.N. Buckley and S.J. Shaibani, *Philos. Mag. Lett.* **55** (1), 15 (1987).
7. Y. Satoh, C. Kinoshita, and K. Nakai, *J. Nucl. Mater.* **179-181**, 399 (1991).
8. S.J. Zinkle, in *Microstructure Evolution During Irradiation*, MRS Symposium Proceedings, edited by I.M. Robertson, G.S. Was, L.W. Hobbs, and T. Diaz de la Rubia (Materials Research Society, Pittsburgh, 1997), Vol. 439, p. 667.
9. S.J. Zinkle, *J. Nucl. Mater.* **219**, 113 (1995).
10. K. Yasuda, C. Kinoshita, R. Morisaki, and H. Abe, *Philos. Mag. A* **78** (3), 583 (1998).
11. A. Tuross, Hj. Matzke, A. Drigo, A. Sambo, and R. Falcone, *Nucl. Instr. Meth. B* **113**, 261 (1996).
12. N. Yu, R. Devanathan, K.E. Sickafus, and M. Nastasi, *J. Mater. Res.* **12** (7), 1766 (1997).
13. S.J. Zinkle and G.P. Pells, *J. Nucl. Mater.* **253**, 120 (1998).
14. N. Bordes, L.M. Wang, R.C. Ewing, and K.E. Sickafus, *J. Mater. Res.* **10** (4), 981 (1995).
15. S.J. Zinkle and L.L. Snead, *Nucl. Instr. Meth. B* **116**, 92 (1996).
16. R. Devanathan, N. Yu, K.E. Sickafus, and M. Nastasi, *Nucl. Instr. Meth. B* **127/128**, 608 (1997).
17. S.X. Wang, L.M. Wang, R.C. Ewing, and R.H. Doremus, *J. Non-Cryst. Solids* **238**, 198 (1998).
18. M. Toulemonde, S. Bouffard, and F. Studer, *Nucl. Instr. Meth. B* **91**, 108 (1994).
19. S.J. Zinkle and V.A. Skuratov, *Nucl. Instr. Meth. B* **141**, 737 (1998).
20. T. Wiss and Hj. Matzke, 19th Int. Conf. on Nuclear Tracks in Solids, to be publ. in *Radiation Measurements*, in press (1999).
21. J.F. Ziegler, J.P. Biersak, and U. Littmark, *The Stopping and Range of Ions in Solids* (Pergamon Press, New York, 1985).
22. S.P. Chen, M. Yan, J.D. Gale et al., *Philos. Mag. Lett.* **73** (2), 51 (1996).
23. B. Canut, A. Benyagoub, G. Marest et al., *Phys. Rev. B* **51** (18), 12194 (1995).
24. P.A. Thevenard, M. Beranger, B. Canut, and S.M.M. Ramos, in *Ion-Solid Interactions for Materials Modification and Processing*, MRS Symposium Proceedings, edited by D.B. Poker, et al. (Materials Research Society, Pittsburgh, 1996), Vol. 396, p. 127.
25. S.M.M. Ramos, N. Bonardi, B. Canut, and S. Della-Negra, *Phys. Rev. B* **57** (1), 189 (1998).
26. R. Devanathan, K.E. Sickafus, N. Yu, and M. Nastasi, *Philos. Mag. Lett.* **72** (3), 155 (1995).
27. N. Chauvin, R.J.M. Konings, and Hj. Matzke, *J. Nucl. Mater.* **in press** (1999).